On the pair-electromagnetic pulse from an electromagnetic black hole surrounded by a baryonic remnant

R. Ruffini[1]**, J.D. Salmonson**[2]**, J.R. Wilson**[2]**, and S.-S. Xue**[1]

[1] University of Rome "La Sapienza", I.C.R.A.-International Center for Relativistic Astrophysics and Physics Department, 00185 Rome, Italy
[2] University of California, Lawrence Livermore National Laboratory, Livermore, California, USA

Abstract. The interaction of an expanding Pair-Electromagnetic pulse (PEM pulse) with a shell of baryonic matter surrounding a Black Hole with electromagnetic structure (EMBH) is analyzed for selected values of the baryonic mass at selected distances well outside the dyadosphere of an EMBH. The dyadosphere, the region in which a super critical field exists for the creation of e^+e^- pairs, is here considered in the special case of a Reissner-Nordstrom geometry. The interaction of the PEM pulse with the baryonic matter is described using a simplified model of a slab of constant thickness in the laboratory frame (constant-thickness approximation) as well as performing the integration of the general relativistic hydrodynamical equations. Te validation of the constant-thickness approximation, already presented in a previous paper Ruffini et al. (1999) for a PEM pulse in vacuum, is here generalized to the presence of baryonic matter. It is found that for a baryonic shell of mass-energy less than 1% of the total energy of the dyadosphere, the constant-thickness approximation is in excellent agreement with full general relativistic computations. The approximation breaks down for larger values of the baryonic shell mass, however such cases are of less interest for observed Gamma Ray Bursts (GRBs). On the basis of numerical computations of the slab model for PEM pulses, we describe (i) the properties of relativistic evolution of a PEM pulse colliding with a baryonic shell; (ii) the details of the expected emission energy and observed temperature of the associated GRBs for a given value of the EMBH mass; $10^3 M_\odot$, and for baryonic mass-energies in the range 10^{-8} to 10^{-2} the total energy of the dyadosphere.

Key words: black hole physics – gamma rays: theory – gamma rays: bursts – gamma rays: observations

1. Introduction

That vacuum polarization process *à la* Heisenberg-Euler-Schwinger (Heisenberg & Euler 1931; Schwinger 1951) can occur in the field of a Kerr Newmann EMBH and that they naturally lead to a model for gamma-ray bursts was pointed out

Send offprint requests to: R. Ruffini (ruffini@icra.it)

in Damour & Ruffini (1975). The basic energetics of the process, governed by the Christodoulou-Ruffini mass formula, for an EMBH gives as shown in Christodoulou & Ruffini (1971),

$$E^2 \;=\; M^2 c^4 = \left(M_{\mathrm{ir}} c^2 + \frac{Q^2}{2\rho_+} \right)^2 + \frac{L^2 c^2}{\rho_+^2}, \tag{1}$$

$$S \;=\; 4\pi \rho_+^2 = 4\pi \left(r_+^2 + \frac{L^2}{c^2 M^2} \right) = 16\pi \left(\frac{G^2}{c^4} \right) M_{\mathrm{ir}}^2, \tag{2}$$

with

$$\frac{1}{\rho_+^4} \left(\frac{G^2}{c^8} \right) \left(Q^4 + 4L^2 c^2 \right) \le 1, \tag{3}$$

where M, L and Q are respectively the mass energy, the angular momentum and the charge of the EMBH and M_{ir} is the irreducible mass, r_+ is the horizon radius, ρ_+ is the quasi-spheroidal cylindrical coordinate of the horizon evaluated at the equatorial plane and S is the horizon surface area. Extreme black holes satisfy the equality in Eq. (3). The vacuum polarization process being "reversible" transformations in the sense of Christodoulou & Ruffini (1971) can extract an energy up to 29% of the mass-energy of an extremal rotating black hole and up to 50% of the mass-energy of an extremely magnetized and charged black hole.

Although in general such a process is endowed with axial symmetry, in order to clarify the pure interplay of the gravitational and electrodynamical phenomena and also for simplicity, we have examined (Ruffini 1998; Preparata et al. 1998a,b) the limiting cases of such a process in the field of a Reissner-Nordstrom geometry whose spherically symmetric metric is given by

$$d^2 s = g_{tt}(r) d^2 t + g_{rr}(r) d^2 r + r^2 d^2 \theta + r^2 \sin^2 \theta d^2 \phi, \tag{4}$$

where $g_{tt}(r) \;=\; -\left[1 - \frac{2GM}{c^2 r} + \frac{Q^2 G}{c^4 r^2} \right] \equiv -\alpha^2(r)$ and $g_{rr}(r) = \alpha^{-2}(r)$. The dyadosphere, defined (see Fig. 1 of Preparata et al. 1998a,b) as the region where the electric field exceeds the critical value, $\mathcal{E}_{\mathrm{c}} = \frac{m^2 c^3}{\hbar e}$ (Heisenberg & Euler 1931; Schwinger 1951), where m and e are the mass and charge of the electron, extends between the horizon radius

$$r_+ \;=\; 1.47 \cdot 10^5 \mu (1 + \sqrt{1 - \xi^2}) \text{ cm.} \tag{5}$$

where we have introduced the dimensionless mass and charge parameters $\mu = \frac{M}{M_\odot}$, $\xi = \frac{Q}{(M\sqrt{G})} \leq 1$, and the outer radius

$$r_{\mathrm{ds}} = 1.12 \cdot 10^8 \sqrt{\mu\xi} \ \mathrm{cm}. \tag{6}$$

Consequently the local number density of electron and positron pairs created in the dyadosphere as a function of radius

$$n_{e^+e^-}(r) = \frac{Q}{4\pi r^2 \left(\frac{\hbar}{mc}\right) e} \left[1 - \left(\frac{r}{r_{\mathrm{ds}}}\right)^2\right], \tag{7}$$

and their energy density is given by

$$\epsilon(r) = \frac{Q^2}{8\pi r^4} \left(1 - \left(\frac{r}{r_{\mathrm{ds}}}\right)^4\right), \tag{8}$$

(see Figs. 2 & 3 of Preparata et al. 1998a,b). The total energy of pairs converted from the static electric energy and deposited within the dyadosphere is then

$$E_{\mathrm{dya}} = \frac{1}{2}\frac{Q^2}{r_+}(1 - \frac{r_+}{r_{\mathrm{ds}}}) \left[1 - \left(\frac{r_+}{r_{\mathrm{ds}}}\right)^2\right], \tag{9}$$

and the total number of electron and position pairs in the dyadosphere is

$$N^\circ_{e^+e^-} \simeq \frac{Q - Q_c}{e} \left[1 + \frac{(r_{\mathrm{ds}} - r_+)}{\frac{\hbar}{mc}}\right], \tag{10}$$

where $Q_c = \mathcal{E}_c r_+^2$ (see Preparata et al. 1998a,b). In the limit of $\frac{r_+}{r_{\mathrm{ds}}} \to 0$, Eq. (9) leads to $E_{\mathrm{dya}} \to \frac{1}{2}\frac{Q^2}{r_+}$, which coincides with the energy extractable from EMBHs by reversible processes ($M_{\mathrm{ir}} = \mathrm{const.}$), namely $E - M_{\mathrm{ir}} = \frac{1}{2}\frac{Q^2}{r_+}$ (see Fig. 4 of Preparata et al. 1998a,b).

Due to the very large pair density given by Eq. (7) and to the sizes of the cross-sections for the process $e^+e^- \leftrightarrow \gamma + \gamma$, the system is expected to thermalize to a plasma configuration for which

$$N_{e^+} = N_{e^-} \sim N_\gamma \sim N^\circ_{e^+e^-}, \tag{11}$$

where $N^\circ_{e^+e^-}$ is the number of e^+e^--pairs created in the dyadosphere (see Preparata et al. 1998a,b). These are the initial conditions for the evolution of the dyadosphere. In a previous paper (Ruffini et al. 1999) we presented the temporal evolution of the dyadosphere in vacuum giving origin to an extremely sharply defined and extremely relativistic expanding pulse of pair and electromagnetical radiation of a constant length in the laboratory frame: the PEM pulse. In this paper we present results of the collision of the PEM pulse with a remnant of baryonic matter surrounding the just formed black hole. We assume the PEM pulse to collide with a shell of baryonic matter of constant density and at a radius of the order of 100 times the radius of the dyadosphere r_{ds} Eq. (6). The shells have this thickness of the order of 10 times r_{ds}. The ass-energies of the shells are taken to be $10^{-8} - 10^{-2}$ of the total energy of the dyadosphere.

The work contains the following sections: Sect. 2 presents discussions of the hydrodynamical equations of a PEM pulse interacting with the baryonic shell; Sect. 3 defines the parameters of the baryonic shells, the behaviour of the PEM pulse colliding with a baryon shell as well as before and after the collision are presented; in Sect. 4 the results of a numerical calculation solving the hydrodynamical equations of Sect. 2 are compared to the results of the analytical model of slab approximation for selected parameters.

2. General relativistic hydrodynamical equations for PEM pulse in presence of baryonic matter

The evolution of the PEM pulse in vacuum was treated in a previous work (Ruffini et al. 1999). We here generalize that treatment to the case in which baryonic matter is present and we outline the relevant relativistic hydrodynamic equations. As in the previous treatment (Ruffini et al. 1999), we assume the plasma fluid of e^+e^--pairs, photons and baryonic matter to be described by the stress-energy tensor

$$T^{\mu\nu} = pg^{\mu\nu} + (p + \rho)U^\mu U^\nu \tag{12}$$

where ρ and p are respectively the total proper energy density and pressure in the comoving frame of the plasma fluid. The U^μ is the four-velocity of the plasma fluid. We have

$$g_{tt}(U^t)^2 + g_{rr}(U^r)^2 = -1, \tag{13}$$

where U^r and U^t are the radial and temporal contravariant components of the 4-velocity. The conservation law of baryon number can be expressed as a function of the proper baryon number density n_B

$$\begin{aligned}
(n_B U^\mu)_{;\mu} &= g^{-\frac{1}{2}}(g^{\frac{1}{2}} n_B U^\nu)_{,\nu} \\
&= (n_B U^t)_{,t} + \frac{1}{r^2}(r^2 n_B U^r)_{,r} = 0. \tag{14}
\end{aligned}$$

The radial component of the energy-momentum conservation law of the plasma fluid reduces to

$$\begin{aligned}
\frac{\partial p}{\partial r} + \frac{\partial}{\partial t}\left((p + \rho)U^t U_r\right) + \frac{1}{r^2}\frac{\partial}{\partial r}\left(r^2(p + \rho)U^r U_r\right) \\
- \frac{1}{2}(p + \rho)\left[\frac{\partial g_{tt}}{\partial r}(U^t)^2 + \frac{\partial g_{rr}}{\partial r}(U^r)^2\right] = 0. \tag{15}
\end{aligned}$$

The component of the energy-momentum conservation law of the plasma fluid equation along a flow line is

$$\begin{aligned}
U_\mu(T^{\mu\nu})_{;\nu} &= -(\rho U^\nu)_{;\nu} - p(U^\nu)_{;\nu}, \\
&= -g^{-\frac{1}{2}}(g^{\frac{1}{2}}\rho U^\nu)_{,\nu} - pg^{-\frac{1}{2}}(g^{\frac{1}{2}}U^\nu)_{,\nu} \\
&= (\rho U^t)_{,t} + \frac{1}{r^2}(r^2 \rho U^r)_{,r} \\
&\quad + p\left[(U^t)_{,t} + \frac{1}{r^2}(r^2 U^r)_{,r}\right] = 0. \tag{16}
\end{aligned}$$

Defining the total proper internal energy density ϵ and the baryonic mass density ρ_B in the comoving frame of the plasma fluid,

$$\epsilon \equiv \rho - \rho_B, \qquad \rho_B \equiv n_B mc^2, \tag{17}$$

and using the law of baryon-number conservation (14), from Eq. (16) we have

$$(\epsilon U^\nu)_{;\nu} + p(U^\nu)_{;\nu} = 0. \tag{18}$$

Recalling that $\frac{dV}{d\tau} = V(U^\mu)_{;\mu}$, where V is the comoving volume and τ is the proper time for the plasma fluid, we have along each flow line

$$\frac{d(V\epsilon)}{d\tau} + p\frac{dV}{d\tau} = \frac{dE}{d\tau} + p\frac{dV}{d\tau} = 0, \tag{19}$$

where $E = V\epsilon$ is total proper internal energy of the plasma fluid. We represent the equation of state by the introduction of a thermal index $\Gamma(\rho, T)$

$$\Gamma = 1 + \frac{p}{\epsilon}. \tag{20}$$

We now turn to the analysis of e^+e^- pairs initially created in the dyadosphere and ionized electrons contained in the baryonic matter. Let n_{e^-} and n_{e^+} be the proper number densities of electrons and positrons associated to pairs created, and $n_{e^-}^b$ the proper number densities of ionized electrons, we clearly have

$$n_{e^-} = n_{e^+} = n_{\text{pair}}, \qquad n_{e^-}^b = \bar{Z}n_B, \tag{21}$$

where n_{pair} is the number of e^+e^- pairs and $\bar{Z}$ the average atomic number $\frac{1}{2} < \bar{Z} < 1$ ($\bar{Z} = 1$ for hydrogen atom and $\bar{Z} = \frac{1}{2}$ for general baryonic matter). The rate equation for electrons and positrons gives,

$$\begin{aligned}
(n_{e^+}U^\mu)_{;\mu} &= (n_{e^+}U^t)_{,t} + \frac{1}{r^2}(r^2 n_{e^+}U^r)_{,r} \\
&= \overline{\sigma v}\big[(n_{e^-}(T) + n_{e^-}^b(T))n_{e^+}(T) \\
&\quad - (n_{e^-} + n_{e^-}^b)n_{e^+}\big],
\end{aligned} \tag{22}$$

$$\begin{aligned}
(n_{e^-}U^\mu)_{;\mu} &= (n_{e^-}U^t)_{,t} + \frac{1}{r^2}(r^2 n_{e^-}U^r)_{,r} \\
&= \overline{\sigma v}\left[n_{e^-}(T)n_{e^+}(T) - n_{e^-}n_{e^+}\right],
\end{aligned} \tag{23}$$

$$\begin{aligned}
(n_{e^-}^b U^\mu)_{;\mu} &= (n_{e^-}^b U^t)_{,t} + \frac{1}{r^2}(r^2 n_{e^-}^b U^r)_{,r} \\
&= \overline{\sigma v}\left[n_{e^-}^b(T)n_{e^+}(T) - n_{e^-}^b n_{e^+}\right],
\end{aligned} \tag{24}$$

where $\overline{\sigma v}$ is the mean of the product of the annihilation cross-section and the thermal velocity of the electrons and positrons, $n_{e^\pm}(T)$ are the proper number densities of electrons and positrons associated to the pairs, given by appropriate Fermi integrals with zero chemical potential, and $n_{e^-}^b(T)$ is the proper number density of ionized electrons, given by appropriate Fermi integrals with non-zero chemical potential μ_e, at an appropriate equilibrium temperature T. These rate equations can be reduced to

$$\begin{aligned}
(n_{e^\pm}U^\mu)_{;\mu} &= (n_{e^\pm}U^t)_{,t} + \frac{1}{r^2}(r^2 n_{e^\pm}U^r)_{,r} \\
&= \overline{\sigma v}\big[n_{e^-}(T)n_{e^+}(T) - n_{e^-}n_{e^+}\big],
\end{aligned} \tag{25}$$

$$(n_{e^-}^b U^\mu)_{;\mu} = (n_{e^-}^b U^t)_{,t} + \frac{1}{r^2}(r^2 n_{e^-}^b U^r)_{,r} = 0, \tag{26}$$

$$Frac \equiv \frac{n_{e^\pm}}{n_{e^\pm}(T)} = \frac{n_{e^-}^b(T)}{n_{e^-}^b}. \tag{27}$$

Eq. (26) is just the baryon-number conservation law (14) and (27) is a relationship obeyed $n_{e^\pm}, n_{e^\pm}(T)$ and $n_{e^-}^b, n_{e^-}^b(T)$.

The equilibrium temperature T is determined by the thermalization processes occurring in the expanding plasma fluid

with a total proper energy density ρ, governed by the hydrodynamical equations (14,15,16). We have

$$\rho = \rho_\gamma + \rho_{e^+} + \rho_{e^-} + \rho_{e^-}^b + \rho_B, \tag{28}$$

where ρ_γ is the photon energy density, $\rho_B \simeq m_B c^2 n_B$ is the baryonic mass density which is considered to be non relativistic in the range of temperature T under consideration, and $\rho_{e^\pm}$ is the proper energy density of elec trons and positrons pairs given by,

$$\rho_{e^\pm} = \frac{n_{e^\pm}}{n_{e^\pm}(T)}\rho_{e^\pm}(T), \tag{29}$$

where $n_{e^\pm}$ is obtained by integration of Eq. (25) and $\rho_{e^\pm}(T)$ is the proper energy density of electrons(positrons) obtained from zero chemical potential Fermi integrals at the equilibrium temperature T. Whereas, $\rho_{e^-}^b$ is the energy density of the ionized electrons, obtained by the ionization of baryonic matter,

$$\rho_{e^-}^b = \frac{n_{e^-}^b}{n_{e^-}^b(T)}\rho_{e^-}^b(T), \tag{30}$$

where $n_{e^-}^b$ is obtained by integration of Eq. (26) and $\rho_{e^-}(T)$ is the proper energy density of ionized electrons obtained from an appropriate Fermi integral of non-zero chemical potential μ_e at the equilibrium temperature T.

Having intrinsically defined the equilibrium temperature T in Eq. (28), we can also, analogously, evaluate the total pressure

$$p = p_\gamma + p_{e^+} + p_{e^-} + p_{e^-}^b + p_B, \tag{31}$$

where p_γ is the photon pressure, $p_{e^\pm}$ and $p_{e^-}^b$ given by,

$$p_{e^\pm} = \frac{n_{e^\pm}}{n_{e^\pm}(T)}p_{e^\pm}(T), \tag{32}$$

$$p_{e^-}^b = \frac{n_{e^-}^b}{n_{e^-}^b(T)}p_{e^-}^b(T), \tag{33}$$

where the pressures $p_{e^\pm}(T)$ are determined by zero chemical potential Fermi integrals, and $p_{e^-}^b(T)$ is the pressure of the ionized electrons, evaluated by an appropriate Fermi integral of non-zero chemical potential μ_e at the equilibrium temperature T. In Eq. (31), the ions pressure p_B is negligible by comparison with the pressures $p_{\gamma, e^\pm, e^-}(T)$, since baryons and ions are expected to be non-relativistic in the range of temperature T under consideration. Finally, using Eqs. (28,31), we compute the thermal factor Γ of the equation of state (20). The calculation is continued as the plasma fluid expands, cools and the e^+e^- pairs recombine, until it becomes optically thin:

$$\int_R dr(n_{e^\pm} + \bar{Z}n_B)\sigma_T \simeq O(1), \tag{34}$$

where $\sigma_T = 0.665 \cdot 10^{-24}\text{cm}^2$ is the Thomson cross-section and the integration is over the radial interval of the PEM-pulse in the comoving frame. At this point the energy is virtually entirely in the form of free-streaming photons and the calculation is stopped.

3. The quasi-analytical simplified model based on the constant-thickness approximation

The PEM pulse expansion in the absence of baryonic matter has been discussed in a previous paper (Ruffini et al. 1999) where the quasi-analytical approach of an expanding shell of constant thickness in the laboratory frame was adopted and validated by comparison with the numerical integration of the general relativistic hydrodynamical equations. We here generalize these results by examining the collision of the PEM pulse with baryonic matter and adopting the constant-thickness approximation both for the description of the collision and the further expansion of the PEM pulse by a simplified approach to the system of equations outlined in the previous paragraph.

We first recall the main results of the PEM pulse expanding in vacuum: we indicate by $U(r) = U_r = $ const. the four-velocity of the slab and by $\mathcal{D} = r_{\rm ds} - r_+$ the constant width of the slab in the laboratory frame of the plasma fluid, the average bulk relativistic gamma-factor $\bar{\gamma}$ is,

$$\bar{\gamma} = \sqrt{1 + U_r^2}, \qquad V_r = \frac{U_r}{\bar{\gamma}}. \tag{35}$$

The evolution of the slab is governed by the total energy and entropy conservations, which are cast into the following equations as a function of the coordinate volume of the plasma fluid expanding from $\mathcal{V}_\circ$ to $\mathcal{V}$,

$$\frac{\bar{\epsilon}_\circ}{\bar{\epsilon}} = \left(\frac{V}{V_\circ}\right)^\Gamma = \left(\frac{\mathcal{V}}{\mathcal{V}_\circ}\right)^\Gamma \left(\frac{\bar{\gamma}}{\bar{\gamma}_\circ}\right)^\Gamma, \tag{36}$$

$$\bar{\gamma} = \bar{\gamma}_\circ \sqrt{\frac{\bar{\epsilon}_\circ \mathcal{V}_\circ}{\bar{\epsilon}\mathcal{V}}}, \tag{37}$$

$$\frac{\partial}{\partial t}(N_{e\pm}) = -N_{e\pm}\frac{1}{\mathcal{V}}\frac{\partial \mathcal{V}}{\partial t} + \overline{\sigma v}\frac{1}{\bar{\gamma}^2}(N_{e\pm}^2(T) - N_{e\pm}^2), \tag{38}$$

where the proper volume V of the plasma fluid $V = \bar{\gamma}\mathcal{V}$ and the thermal index Γ Eq. (20), a slowly-varying function of the state with values around 4/3, has been approximately assumed to be constant. The coordinate number density of $e^\pm$-pairs in equilibrium is $N_{e\pm}(T) \equiv \bar{\gamma}n_{e\pm}(T)$ and the coordinate number density of $e^\pm$-pairs $N_{e\pm} \equiv \bar{\gamma}n_{e\pm}$. These equations have already been numerically integrated (Ruffini et al. 1999).

The baryonic matter remnant is assumed to be distributed well outside the dyadosphere in a shell of thickness Δ between an inner radius $r_{\rm in}$ and an outer radius $r_{\rm out}$ at a distance from the EMBH at which the original PEM pulse expanding in vacuum has not yet reached transparency,

$$r_{\rm in} = 100 r_{\rm ds}, \qquad \Delta = 10 r_{\rm ds}, \qquad r_{\rm out} = r_{\rm in} + \Delta. \tag{39}$$

The total baryonic mass ($M_B = N_B m_p c^2$) is assumed to be a fraction of the dyadosphere initial total energy ($E_{\rm dya}$). The total baryon-number (N_B) is then given by

$$N_B = B\frac{E_{\rm dya}}{m_p c^2}. \tag{40}$$

where B is a parameter in the range $10^{-8} - 10^{-2}$ and where m_p is the proton mass. The baryon number density n_B° is assumed to be a constant,

$$\bar{n}_B^\circ = \frac{N_B}{V_B}, \qquad \bar{\rho}_B^\circ = m_p \bar{n}_B^\circ. \tag{41}$$

As the PEM pulse reaches the region $r_{\rm in} < r < r_{\rm out}$, it interacts with the baryonic matter which is assumed to be at rest. In our simplified quasi-analytic model we make the following assumptions to describe this interaction:

– the PEM pulse does not change its geometry during the interaction;
– the collision between the PEM pulse and the baryonic matter is assumed to be inelastic,
– the baryonic matter reaches thermal equilibrium with the photons and pairs of the PEM pulse.

These assumptions are valid if: (i) the total energy of the PEM pulse is much larger than the total mass-energy of baryonic matter M_B, $10^{-8} < E_{\rm dya}/M_B < 10^{-2}$, and (ii) the comoving number density ratio $n_{e^+e^-}/n_B^\circ$ of pairs and baryons at the moment of collision is extremely high (e.g., $10^6 < n_{e^+e^-}/n_B^\circ < 10^{12}$, and (iii) the PEM pulse has a large value of Lorentz factor ($600 < \bar{\gamma} < 4000$).

In the collision process between the PEM pulse and the baryonic matter at $r_{\rm out} > r > r_{\rm in}$, we impose the total energy and momentum conservations. We consider the collision process between two radii r_2, r_1, satisfying $r_{\rm out} > r_2 > r_1 > r_{\rm in}$ and $r_2 - r_1 \ll \Delta$. The amount of baryonic mass acquired by the PEM pulse is

$$\Delta M = \frac{M_B}{V_B}\frac{4\pi}{3}(r_2^3 - r_1^3), \tag{42}$$

where M_B/V_B is the mean-density of baryonic matter at rest. The conservation of total energy leads to the estimate of the corresponding quantities before (with "$\circ$") and after such a collision

$$(\Gamma\bar{\epsilon}_\circ + \bar{\rho}_B^\circ)\bar{\gamma}_\circ^2\mathcal{V}_\circ + \Delta M = (\Gamma\bar{\epsilon} + \bar{\rho}_B + \frac{\Delta M}{V} + \Gamma\Delta\bar{\epsilon})\bar{\gamma}^2\mathcal{V}, \tag{43}$$

where $\Delta\bar{\epsilon}$ is the corresponding increase of internal energy due to the collision. Similarly the momentum-conservation gives

$$(\Gamma\bar{\epsilon}_\circ + \bar{\rho}_B^\circ)\bar{\gamma}_\circ U_r^\circ\mathcal{V}_\circ = (\Gamma\bar{\epsilon} + \bar{\rho}_B + \frac{\Delta M}{V} + \Gamma\Delta\bar{\epsilon})\bar{\gamma}U_r\mathcal{V}, \tag{44}$$

where radial component of the four-velocities of the PEM pulse $U_r^\circ = \sqrt{\bar{\gamma}_\circ^2 - 1}$ and Γ thermal index. We then find

$$\Delta\bar{\epsilon} = \frac{1}{\Gamma}\left[(\Gamma\bar{\epsilon}_\circ + \bar{\rho}_B^\circ)\frac{\bar{\gamma}_\circ U_r^\circ\mathcal{V}_\circ}{\bar{\gamma}U_r\mathcal{V}} - (\Gamma\bar{\epsilon} + \bar{\rho}_B + \frac{\Delta M}{V})\right], \tag{45}$$

$$\bar{\gamma} = \frac{a}{\sqrt{a^2 - 1}}, \qquad a \equiv \frac{\bar{\gamma}_\circ}{U_r^\circ} + \frac{\Delta M}{(\Gamma\bar{\epsilon}_\circ + \bar{\rho}_B^\circ)\bar{\gamma}_\circ U_r^\circ\mathcal{V}_\circ}. \tag{46}$$

These equations determine the gamma-factor $\bar{\gamma}$ and the internal energy density $\bar{\epsilon} = \bar{\epsilon}_\circ + \Delta\bar{\epsilon}$ in the capture process of baryonic matter by the PEM pulse. After collision ($r > r_{\rm out}$), the
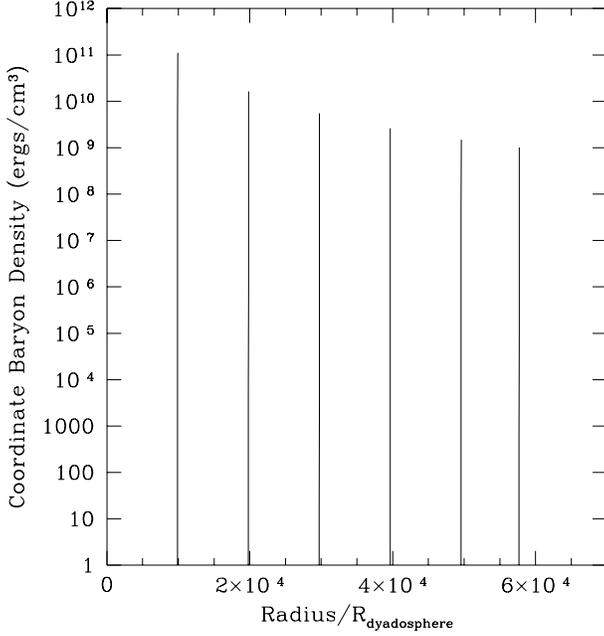
Fig. 1. A sequence of snapshots of coordinate baryon energy density is shown from the one-dimensional (1-D) hydrodynamic calculations. This run corresponds to the $M_{\mathrm{BH}} = 10^3 M_\odot, \xi = 0.1$ EMBH and $B = 1.3 \cdot 10^{-4}$ baryonic shell. The spikes are actually narrow, unresolved shells (see Fig. 2).

further adiabatic expansion of PEM pulse is described by the total baryon number, energy and entropy conservations, i.e., the following hydrodynamical equations which generalize those derived in our previous paper (Ruffini et al. 1999) with $\rho_B \neq 0$,

$$\frac{\bar{n}_B^\circ}{\bar{n}_B} = \frac{V}{V_\circ} = \frac{\mathcal{V}\bar{\gamma}}{\mathcal{V}_\circ\bar{\gamma}_\circ}, \tag{47}$$

$$\frac{\bar{\epsilon}_\circ}{\bar{\epsilon}} = \left(\frac{V}{V_\circ}\right)^\Gamma = \left(\frac{\mathcal{V}}{\mathcal{V}_\circ}\right)^\Gamma \left(\frac{\bar{\gamma}}{\bar{\gamma}_\circ}\right)^\Gamma, \tag{48}$$

$$\bar{\gamma} = \bar{\gamma}_\circ \sqrt{\frac{(\Gamma\bar{\epsilon}_\circ + \rho_B^\circ)\mathcal{V}_\circ}{(\Gamma\bar{\epsilon} + \bar{\rho}_B)\mathcal{V}}}, \tag{49}$$

$$\frac{\partial}{\partial t}(N_{e\pm}) = -N_{e\pm}\frac{1}{\mathcal{V}}\frac{\partial\mathcal{V}}{\partial t} + \overline{\sigma v}\frac{1}{\bar{\gamma}^2}(N_{e\pm}^2(T) - N_{e\pm}^2). \tag{50}$$

In these equations $(r > r_{\mathrm{out}})$ the comoving baryonic mass- and number densities are $\bar{\rho}_B = M_B/V$ and $\bar{n}_B = N_B/V$, where V is the comoving volume of the PEM pulse. The integration is continued untill the transparency condition in Eq. (34) is reached.

4. Validation of the constant-thickness approximation

The numerical integration of the general relativistic equations given in Sect. 2 have already been presented in a series of papers (see Wilson 1975, 1977; Wilson et al. 1996). We can then proceed to compare and contrast the results obtained by the numerical integration of the Eqs. (14)-(16) and the simplified quasi-analytical approach given by Eq. (36)-(38), (43)-(44) and (47)-
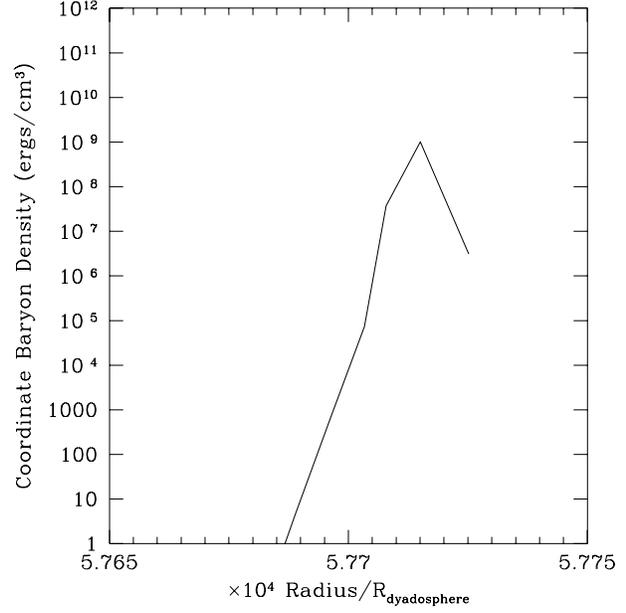

Fig. 2. A detail of the last shell of the previous Fig. 1. In this figure the thickness of the shell is resolved.

(50). We select the specific example of an EMBH of $10^3 M_\odot$ with a charge-to-mass ratio $\xi = 0.1$. From the equations already published (Preparata et al. 1998a,b), the total energy in the dyadosphere is $3.09 \cdot 10^{54}$ergs. The PEM pulse is assumed to collide with a baryonic shell of thickness $\Delta = 10 r_{\mathrm{ds}}$ at rest at a radius of $100 r_{\mathrm{ds}}$. We have considered five different cases: (1) a shell of baryonic mass $2.23 \cdot 10^{-4} M_\odot$ ($4 \cdot 10^{50}$ ergs rest energy), from corresponding to a parameter $B \simeq 1.3 \cdot 10^{-4}$; (2) $6.7 \cdot 10^{-4} M_\odot$ ($1.2 \cdot 10^{51}$ ergs, $B \simeq 3.8 \cdot 10^{-4}$); (3) $2.2 \cdot 10^{-3} M_\odot$ ($4 \cdot 10^{51}$ ergs, $B \simeq 1.3 \cdot 10^{-3}$); (4) $6.7 \cdot 10^{-3} M_\odot$ ($1.2 \cdot 10^{52}$ ergs, $B \simeq 3.8 \cdot 10^{-3}$); (5) $2.2 \cdot 10^{-2} M_\odot$ ($4 \cdot 10^{52}$ ergs, $B \simeq 1.3 \cdot 10^{-3}$). The collision between the expanding slab and the baryonic matter shell is treated as an inelastic collision in both calculations.

We first proceed to a qualitative analysis of the evolution of the PEM pulse in Eqs. (14)-(16) from Figs. 1,2 corresponding to $B \simeq 1.3 \cdot 10^{-4}$ and Figs. 3,4,5 corresponding to $B \simeq 3.8 \cdot 10^{-4}, 1.3 \cdot 10^{-3}, 3.8 \cdot 10^{-3}$, we see that the PEM pulse after collision with the baryonic matter shell continues to expand as a one dimensional slab. We see, however, from Figs. 6 corresponding to $B \simeq 1.3 \cdot 10^{-2}$ that the expansion after collision becomes much more complex and the constant-thickness approximation ceases to be valid. From this qualitative analysis we now proceed to a quantitative analysis in Fig. 7. We compare and contrast the bulk gamma factor as computed from the constant-thickness approximation and the one from the full set of Eqs. (14)-(16). The computation refers to the case $B \simeq 1.3 \cdot 10^{-4}$ where an excellent qualitative agreement with the one-dimensional-slab approximation has been found. The extremely good agreement validates the constant-thickness approximation. This agreement has been found up to values of B no larger than 10^{-2}.
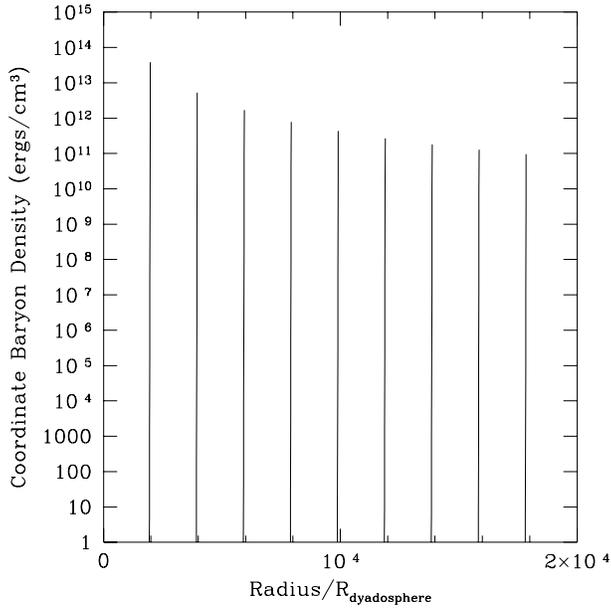
Fig. 3. As in Fig. 1 with the $M_{\mathrm{BH}} = 10^3 M_\odot, \xi = 0.1$ EMBH and $B = 3.8 \cdot 10^{-4}$ baryonic shell.
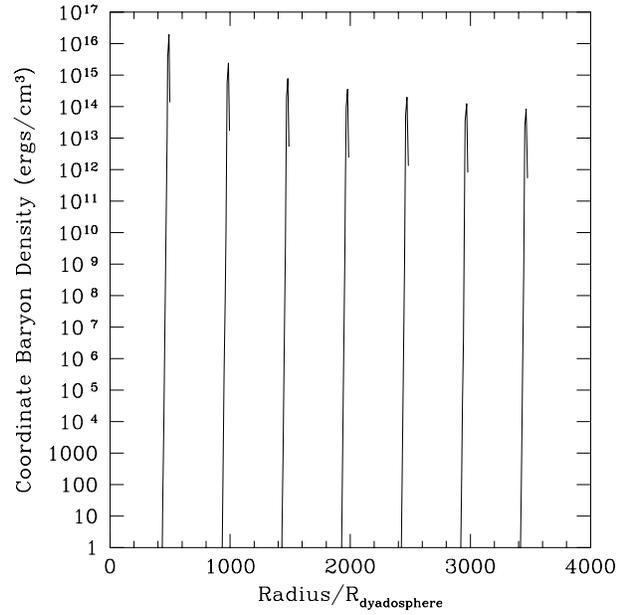

Fig. 5. As in Fig. 1 with the $M_{\mathrm{BH}} = 10^3 M_\odot, \xi = 0.1$ EMBH and $B = 3.8 \cdot 10^{-3}$ baryonic shell.
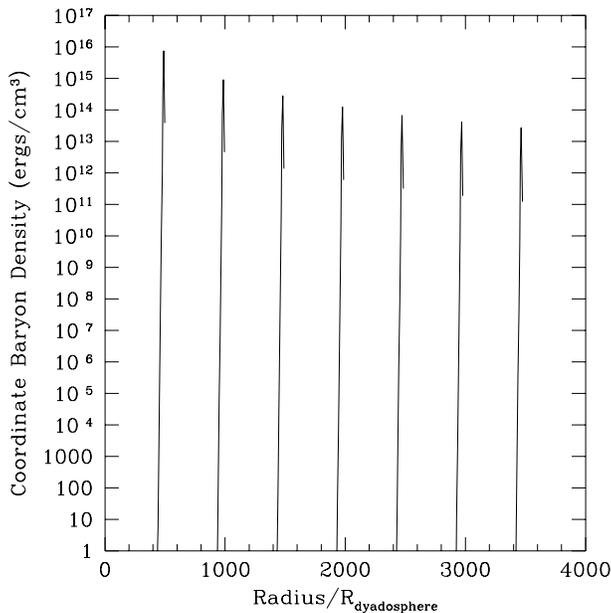

Fig. 4. As in Fig. 1 with the $M_{\mathrm{BH}} = 10^3 M_\odot, \xi = 0.1$ EMBH and $B = 1.3 \cdot 10^{-3}$ baryonic shell.
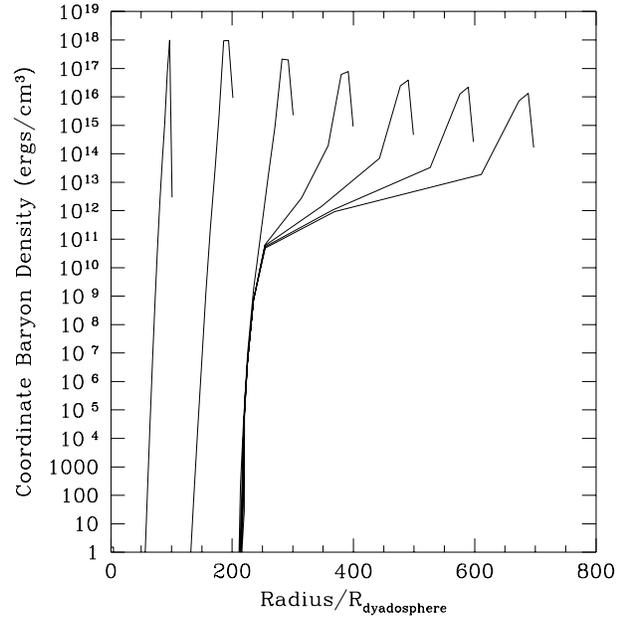

Fig. 6. As in Fig. 1 with the $M_{\mathrm{BH}} = 10^3 M_\odot, \xi = 0.1$ EMBH and $B = 1.3 \cdot 10^{-2}$ baryonic shell. For this baryon shell mass we see a significant departure from the behavior seen in Figs. 1, 3, 4, 5. The baryon shell mass is significant enough to distort the PEM pulse shell. Thus the PEM pulse can no longer be reliably modeled as a shell of constant coordinate thickness and the comparison of Fig. 7 can no longer be made.

5. Considerations on the GRB structures descending from a constant-thickness approximation

We now proceed to some specific prediction of GRB features computed by using the constant-thickness approximation and the Eqs. (36)-(38), (43)-(44) and (47)-(50) in the range of validation of this approximation just defined in the previous paragraph. As an example for clearly showing the evolution of PEM pulses colliding with baryonic matter, we take the following

black hole mass and charge, as well as the mass of baryon remnant as a typical case:

$$M_{\mathrm{BH}} = 10^3 M_\odot, \quad \xi = 0.1, \quad M_B = 10^{-2} E_{\mathrm{dya}}, \quad (51)$$

where the total energy of dyadosphere $E_{\mathrm{dya}} = 3.09 \cdot 10^{54}$ ergs, so the total number of $e^+ e^-$-pairs created in the dyadosphere
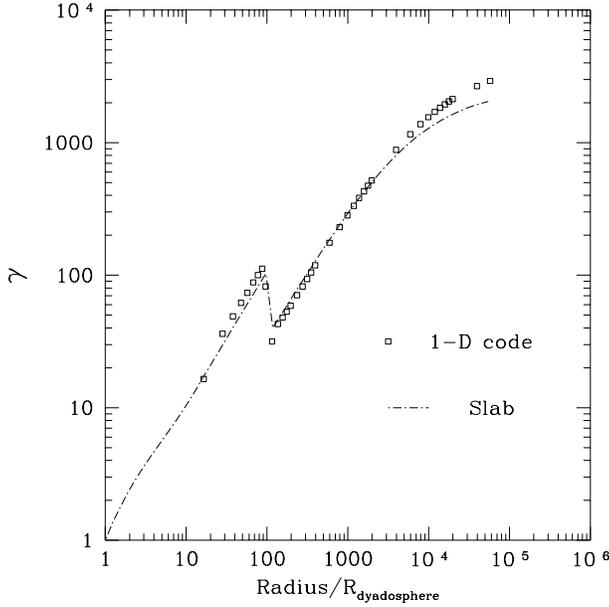
Fig. 7. Here we see a comparison of Lorentz factor γ for the one-dimensional (1-D) hydrodynamic calculations and slab calculations ($M_{\mathrm{BH}} = 10^3 M_\odot, \xi = 0.1$ EMBH and $B \simeq 1.3 \cdot 10^{-4}$). The calculations show good agreement.

Fig. 8. The Lorentz factors are given, as functions of the radius, in units of the dyadosphere radius, for selected values of shell masses given by $B \equiv (M_B c^2)/E_{\mathrm{dya}}$ for the typical case $M_{\mathrm{BH}} = 10^3 M_\odot, \xi = 0.1$. The asymptotic values $\gamma_{\mathrm{asym}} = E_{\mathrm{dya}}/(M_B c^2) = 10^4, 10^3, 10^2$ are also plotted.

(given by Eq. (10)) $N^\circ_{e^+ e^-} = 1.9 \cdot 10^{60}$, and baryonic mass $M_B = 1.73 \cdot 10^{-2} M_\odot$. This baryonic mass is close to the limit of validation of the slab model shown in Sect. 4. We have assumed the baryonic matter at a distance of $r_{\mathrm{in}} = 100 r_{\mathrm{ds}}$, very close to the transparency condition of the PEM pulse in vacuum (see Ruffini et al. 1999).

In Fig. 8 we represent the Lorentz Factor of the PEM pulse as a function of the radius for collision with different amounts of baryonic matter, corresponding respectively to $B = 10^{-2}$, $B = 10^{-3}$ and $B = 10^{-4}$. The diagram extends to values of the radial coordinate at which the transparency condition given by Eq. (34) is reached. Also represented, for each diagram, is the "asymptotic" Lorentz Factor:

$$\bar{\gamma}_{\mathrm{asym}} \equiv \frac{E_{\mathrm{dya}}}{M_B c^2}. \tag{52}$$

The closer the $\bar{\gamma}$ value approaches, at transparency, the "asymptotic" value (52), the smaller the intensity of the radiation emitted in the burst, and the larger the amount of kinetic energy left in the baryonic matter. This point is further clarified in Fig. 9, where are plotted the $\bar{\gamma}$-factor at transparency and the "asymptotic" one as functions of the baryonic matter. It is interesting that, for a given EMBH, there is a maximum value of the $\bar{\gamma}$-factor at transparency. After that maximum value, the energy available for the GRB is smaller in intensity, and at decreasing values of the energy, for increasing values of the baryonic mass.

The temperature in the laboratory frame $\bar{\gamma}T$ at the transparency point is plotted as a function of the baryonic mass in Fig. 10: it strongly decreases as the baryonic mass increase. The $\bar{\gamma}T$ is related to the observed energy-peak of the photon-number spectrum (see e.g., Ruffini et al. 1999).
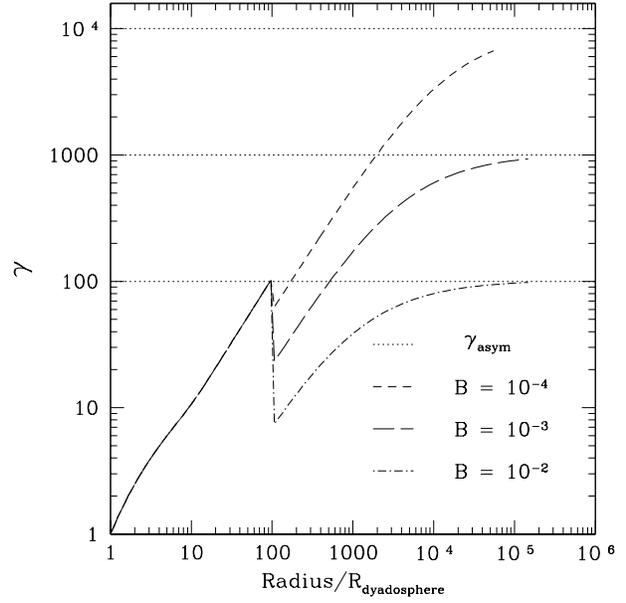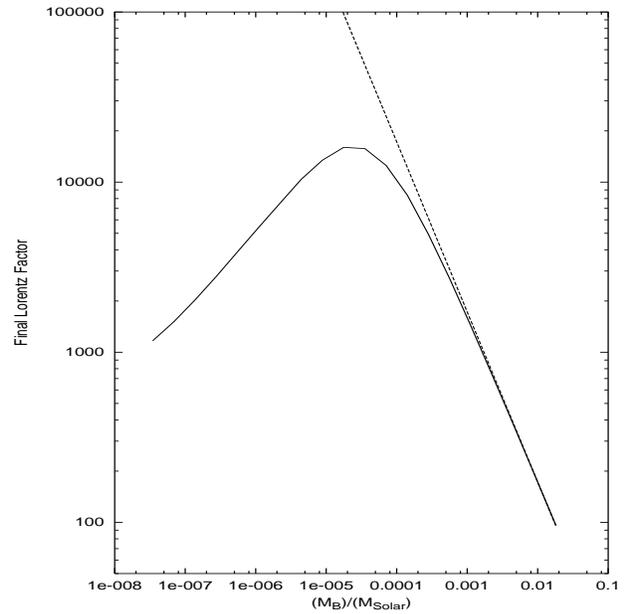

Fig. 9. The final Lorentz-factor (the solid line) at the transparent point is plotted as function of baryonic masses M_B in the unit of the solar mass. The asymptotic value (the dashed line) $E_{\mathrm{dya}}/(M_B c^2)$ is also plotted.

We plot in Fig. 11 the energy radiated in the burst and the final kinetic energy of baryonic matter. We find that, for small values of B (around 10^{-8}), almost all total energy is radiated as GRB (see also our previous paper Ruffini et al. 1999), and very little energy is left as kinetic energy of baryonic matter as afterglow. While for $B \simeq 10^{-2}$ roughly only 10^{-2} of the total
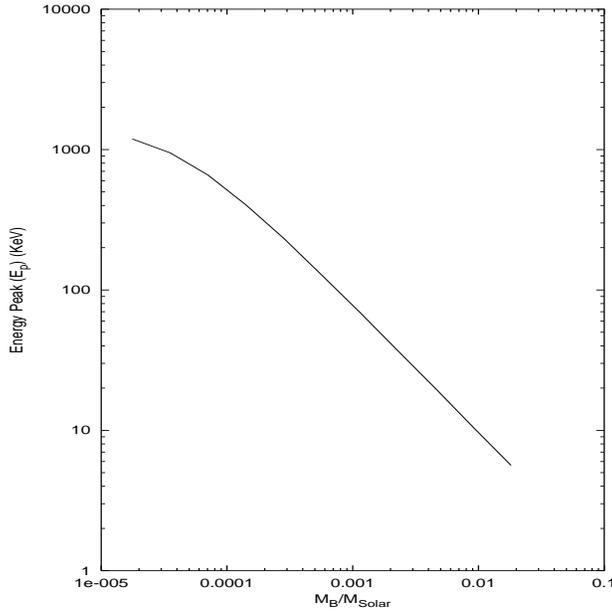
Fig. 10. The observed temperature $E_p \sim \bar{\gamma} T$ in the laboratory frame is plotted as function of baryonic masses $M_B c^2$ in the unit of the solar mass.
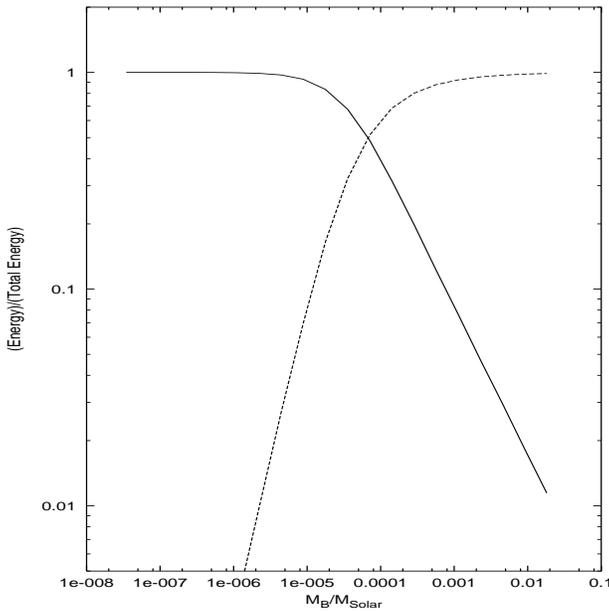

Fig. 11. At the transparent point, the energy radiated in the burst (the solid line) and the final kinetic energy (the dashed line) of baryonic matter, in units of the total energy of the dyadosphere, are plotted as functions of baryonic mass $M_B c^2$ in units of solar mass.

initial energy of the dyadosphere is radiated away as GRB, and almost all energy is restored as the kinetic energy of the baryonic matter. It is also clear that for $B > 10^{-2}$ the intensity of the Burst (see also Fig. 8) and the observed radiation frequency drifted to smaller and smaller values and are of little astrophysical interest from the point of view of GRBs. For such values, the energy of the dyadosphere is transferred practically totally to the bulk kinetic energy of the baryonic matter. $B = 10^{-2}$ is also the limit
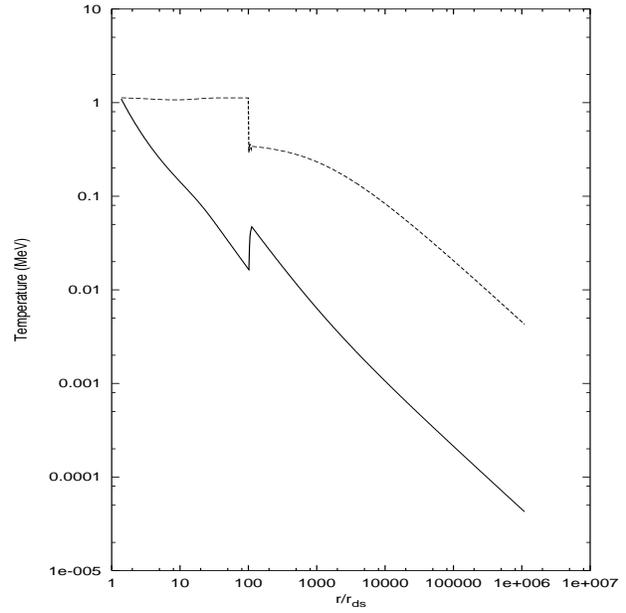

Fig. 12. The temperature in the comoving frame T'(MeV) (the solid line) and in the laboratory frame $\bar{\gamma} T'$ (the dashed line) are plotted as functions of the radius in the unit of the dyadosphere radius r_{ds} for the typical case $M_{BH} = 10^3 M_\odot, \xi = 0.1$ and $B = 10^{-2}$ (see Sect. 5 in the text).

of the validation of our computations based on the analytical slab model, described in Sect. 3. For values of baryonic matter in between these two extreme cases ($B = 10^{-8}$ and $B = 10^{-2}$) the analytical slab model covers the whole range of the observed properties of Gamma Ray Bursts.

We turn now to the thermodynamic parameters relevant in the evolution of the PEM pulse. In Fig. 12 the temperature of PEM pulse, both in the comoving and in the laboratory frame, are given as a function of the radius for a typical case ($M_{BH} = 10^3 M_\odot, \xi = 0.1$ and $B = 10^{-2}$).

In Fig. 13, we plot the total energy of the non baryonic components of the PEM pulse, which includes both thermal and kinetic energy, and the kinetic energy of the baryonic matter as functions of the radius, for the typical case $M_{BH} = 10^3 M_\odot, \xi = 0.1$ and $B = 10^{-2}$. The total energy of the non baryonic components of the PEM pulse is equal to E_{dya} before the collision (see Ruffini et al. 1999) and drops after the collision. While the kinetic energy of baryonic matter

$$E_k = \bar{\rho}_B V (\bar{\gamma} - 1) \tag{53}$$

increases as function of radius for $(r > r_{in})$. The sum of both them is equal to the total energy $E_{dya} = 3.09 \cdot 10^{54}$ergs during the evolution of the PEM pulse. The value of the total energy of the non baryonic components of the PEM pulse at the transparency point, the ending point of the curve in Fig. 13, is the energy released in the burst. We have discussed this energy as function of baryonic masses in Fig. 11.

Before and after the collision, the condition of entropy conservation applies, and we have:

$$S_{before} = \frac{V}{T} \left(\rho_\gamma + \rho_{e\pm} + p_\gamma + p_{(e\pm)} \right) \tag{54}$$
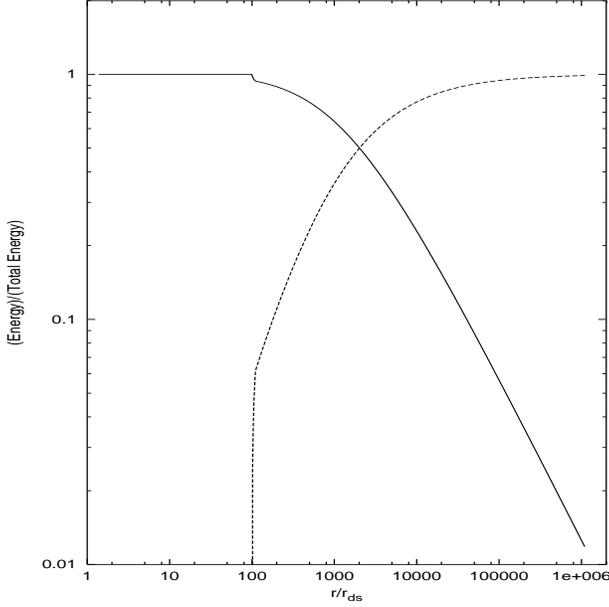
Fig. 13. The total energy of the non baryonic components of the PEM pulse (the solid line) and the total kinetic energy of baryonic matter (the dashed line) in the unit of the total energy are plotted as functions of the radius in the unit of the dyadosphere radius r_{ds} for the typical case $M_{BH} = 10^3 M_\odot, \xi = 0.1$ and $B = 10^{-2}$.

Fig. 14. The number densities $n_{e^+ e^-}(T)$ (the solid line) computed by the Fermi integral and $n_{e^+ e^-}$ (the dashed line) computed by the rate equation (38) are plotted as functions of the radius. $T' \ll m_e c^2$, two curves strongly divergent due to $e^+ e^-$-pairs frozen out of the thermal equilibrium. The peak at $r = r_{ds}$ is due to the temperature reheating in the collision.

$$S_{after} = \frac{V}{T}\left(\rho_\gamma + \rho_{e^\pm} + \rho_{e^-}^b + \epsilon_B \right.$$
$$\left. + p_\gamma + p_{e^\pm} + p_B + p_{e^-}^b \right), \tag{55}$$

where ϵ_B is the thermal energy of baryonic matter, and we can neglect, in Eq. (55), the pressure of the baryonic matter. A sudden increase of the entropy occurs during the collision both for the addition of the baryonic matter, and for the thermal reheating due to the inelastic collapse of the PEM pulse with the baryonic matter at rest. From the energy and momentum conservations, we obtain for the values of the $\bar{\gamma}$ and the temperature during the collision: the proper internal energy, E_{int}, of the plasma increases as

$$dE_{int} = (\gamma - 1)dM_B \tag{56}$$

and the slab is decelerated, in terms of Lorentz factor γ, as

$$d\gamma = -\frac{\gamma^2 - 1}{M_B c^2 + E_{int}}dM_B, \tag{57}$$

as baryon mass, dM_B, is incrementally gained.

Before the collision the PEM pulse expands keeping its temperature in the laboratory frame constant, while its temperature in the comoving frame falls (see Ruffini et al. 1999). During the collision, a heating of the plasma due to the energy and momentum conservation occurs (see also Fig. 14, where reheating process leads to an increment of the number density of $e^+ e^-$ pairs). As the system expands further, both the comoving temperature and the temperature in the laboratory frame decreases, since the total energy of the $e^+ e^-$ pairs and the photons be-
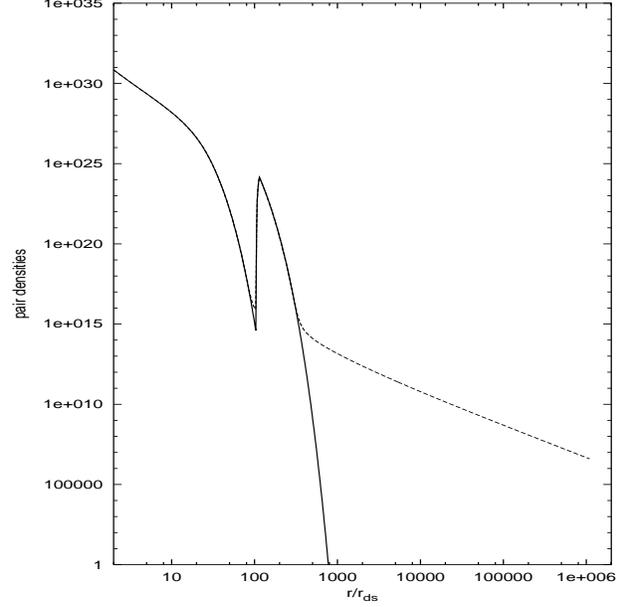
fore the collision is constant and equal to E_{dya}, while after the collision

$$E_{dya} = E_{Baryons} + E_{e^+ e^-} + E_{photons} \tag{58}$$

where $E_{Baryons}$ is only the thermal energy of the baryons.

It is also interesting to monitor the change of temperature in the comoving frame before the collision and after the collision (see also Fig. 15). Before the collision, due to the entropy conservation, in the process of $e^+ e^-$ annihilation the factor $\frac{T^3 V}{T_\circ^3 V_\circ}$ (where the subscript "$\circ$" means "initial value") increases to a value near to $\frac{11}{4}$ (see Weinberg 1972; Ruffini et al. 1999) since the collision occurs at $r = 100 r_{ds}$, near the condition of transparency. The number of $e^+ e^-$ pairs has now been reduced drastically. The further jump in the value of the ratio $\frac{T^3 V}{T_\circ^3 V_\circ}$ is principally due to the energy and momentum conservation during the inelastic collision. After the collision, there is a small reheating due to the annihilation of the $e^+ e^-$ pairs created in the collision (see Fig. 14), which cannot be seen on the scale of our plot. Then, the ratio remains constant.

6. Conclusions

By the direct comparison with the numerical integration of the complete relativistic hydrodynamical equations, the use of the constant-thickness approximation has been validated for values of the parameter $B \leq 10^{-2}$. For $B \geq 10^{-2}$ the amount of energy released at transparency in the burst decreases, and its energy drifts toward low energy values, which are of little interest for the astrophysics of GRB. We
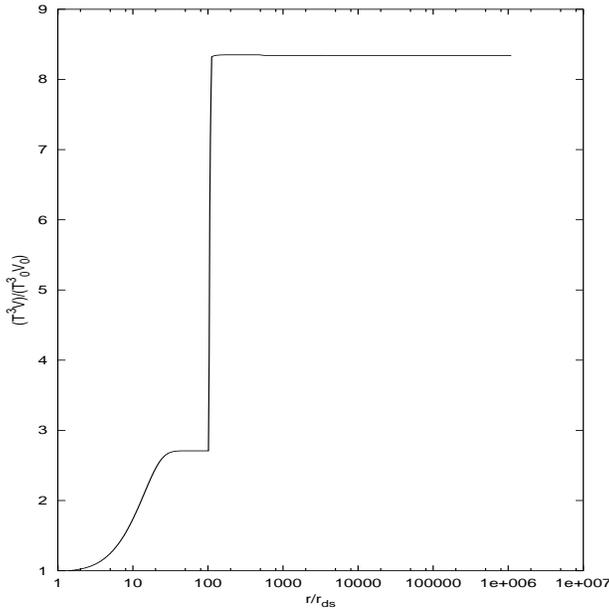
Fig. 15. We plot the ratio $(T^3 V)/(T_\circ^3 V_\circ)$, T being the temperature of the PEM pulse, and V the volume in the comoving frame, as function of the radius in the unit of the dyadosphere radius r_{ds} for the typical case $M_{BH} = 10^3 M_\odot, \xi = 0.1$ and $B = 10^{-2}$ (see Sect. 5 in the text). After the collision, there is a small reheating up to the annihilation of the $e^+ e^-$ pairs recreated in the collision (see Fig. 14), which cannot be seen on the scale of our plot.

conclude that the constant-thickness approximation is valid for all astrophysically relevant situations for the analysis of the GRB at transparency. Based on this validation we have studied the evolution of a PEM pulse in the presence of selected amounts of baryonic matter. We have studied for a typical case of $M_{BH} = 10^3 M_\odot, \xi = 0.1$ EMBH and $B = 10^{-2}$ baryonic shell, the thermal, the bulk Lorentz factor evolution of the PEM pulse as well as the kinetic energy

left over in the baryonic matter after the decoupling of matter and radiation and the emission of the GRB. Additional results corresponding to a larger range of masses and charges of the EMBH and the correlations between the peak energy and the duration of GRBs to be expected in our model will be considered in a future paper, together with the results of analyzing the interaction of the kinetic energy left over in the baryonic matter, after the decoupling of matter and radiation, with the interstellar medium.

References

Christodoulou D., Ruffini R., 1971, Phys. Rev. D 4, 3552
Damour T., Ruffini R., 1975, Phys. Rev. Lett. 35, 463
Heisenberg W., Euler H., 1931, Zeits. Phys. 69, 742
Preparata G., Ruffini R., Xue S.-S., 1998a, submitted to Phys. Rev. Lett
Preparata G., Ruffini R., Xue S.-S., 1998b, A&A 338, L87
Ruffini R., 1998, In: Sato H., Sugiyama N. (eds.) Black Holes and High Energy Astrophysics. Proceedings of the 49th Yamada Conference, Universal Ac. Press Tokyo
Ruffini R., Salmonson J.D., Wilson J.R., Xue S.-S., 1999, A&A 350, 334; A&AS 138, 511-512
Schwinger J., 1951, Phys. Rev. 82, 664
Weinberg S., 1972, Gravitation and Cosmology. John Wiley & Sons, Inc., USA
Wilson J.R., Mathews G.J., Marronetti P., 1996, Phys. Rev. D 54, 1317
Wilson J.R., 1975, Annals of the New York Academy of Sciences 262, 123
Wilson J.R., 1977, In: Ruffini R. (ed.) Proc. of the First Marcel Grossmann Meeting on General Relativity. North-Holland Pub., Amsterdam, p. 393